Farah Lizotte,[1,2] Benoit Denhez,[1,2] Andréanne Guay,[1,2] Nicolas Gévry,[3] Anne Marie Côté,[1,4] and Pedro Geraldes[1,2]

Persistent Insulin Resistance in Podocytes Caused by Epigenetic Changes of SHP-1 in Diabetes

Diabetes 2016;65:3705–3717 | DOI: 10.2337/db16-0254

Poor glycemic control profoundly affects protein expression and the cell signaling action that contributes to glycemic memory and irreversible progression of diabetic nephropathy (DN). We demonstrate that SHP-1 is elevated in podocytes of diabetic mice, causing insulin unresponsiveness and DN. Thus, sustained SHP-1 expression caused by hyperglycemia despite systemic glucose normalization could contribute to the glycemic memory effect in DN. Microalbuminuria, glomerular filtration rate, mesangial cell expansion, and collagen type IV and transforming growth factor-β expression were significantly increased in diabetic *Ins2*$^{+/C96Y}$ mice compared with nondiabetic *Ins2*$^{+/+}$ mice and remained elevated despite glucose normalization with insulin implants. A persistent increase of SHP-1 expression in podocytes despite normalization of systemic glucose levels was associated with sustained inhibition of the insulin signaling pathways. In cultured podocytes, high glucose levels increased mRNA, protein expression, and phosphatase activity of SHP-1, which remained elevated despite glucose concentration returning to normal, causing persistent insulin receptor-β inhibition. Histone posttranslational modification analysis showed that the promoter region of SHP-1 was enriched with H3K4me1 and H3K9/14ac in diabetic glomeruli and podocytes, which remained elevated despite glucose level normalization. Hyperglycemia induces SHP-1 promoter epigenetic modifications, causing its persistent expression and activity and leading to insulin resistance, podocyte dysfunction, and DN.

Diabetic kidney disease is one of the most devastating microvascular complications of diabetes that can lead to end-stage renal disease (1). Hyperglycemia and insulin resistance are believed to be the major risk factors for the development of diabetic nephropathy (DN). The Diabetes Control and Complications Trial (DCCT) demonstrated that intensive blood glucose control reduces the risk of diabetic microvascular complications (nephropathy, retinopathy, and neuropathy) compared with conventional insulin treatment (2). Moreover, the follow-up Epidemiology of Diabetes Interventions and Complications (EDIC) study showed that the cumulative incidence of nephropathy continues to differ between intensive and standard treatment groups for many years despite comparable HbA_{1c} (3,4). To explain this phenomenon, a new concept named hyperglycemic memory has been suggested to explain the persistence of hyperglycemia-induced metabolic derangements after normalization of blood glucose (5).

Podocytes are highly specialized epithelial cells essential for the integrity of the glomerular filtration barrier (6). Podocyte cell death is an early event of DN (7), and decreased glomerular podocyte density is the strongest predictor of DN progression (8). Insulin action itself is important in podocyte biology. Renal disease similar to DN can be observed in patients with a genetic mutation of insulin receptor (IR) signaling (9,10), and several studies have supported a link between insulin resistance and renal pathology in type 1 diabetes. In a clinical study, 14 patients with type 1 diabetes and microalbuminuria had significantly lower glucose disposal during euglycemic-hyperinsulinemic clamp studies than matched control subjects, even after accounting for blood pressure and BMI (11). Moreover, Welsh et al. (12) uncovered the

[1]Research Center of CHU de Sherbrooke and Department of Medicine, Université de Sherbrooke, Sherbrooke, QC, Canada
[2]Division of Endocrinology, Université de Sherbrooke, Sherbrooke, QC, Canada
[3]Department of Biology, Université de Sherbrooke, Sherbrooke, QC, Canada
[4]Department of Nephrology, Université de Sherbrooke, Sherbrooke, QC, Canada
Corresponding author: Pedro Geraldes, pedro.geraldes@usherbrooke.ca.

Received 23 February 2016 and accepted 26 August 2016.

This article contains Supplementary Data online at http://diabetes.diabetesjournals.org/lookup/suppl/doi:10.2337/db16-0254/-/DC1.

importance of insulin action in podocytes, showing that mice depleted of the IR specifically in podocytes developed albuminuria and podocyte loss, which are characteristic of DN pathology. However, the mechanisms of podocyte and kidney insulin unresponsiveness induced by the hyperglycemic memory effect have not been explored.

The regulation of protein tyrosine phosphatase, such as SHP-1, is an important mechanism for developmental control and homeostasis of an array of cellular processes, including cell growth, differentiation, and oncogenic transformation. SHP-1 is a cytosolic tyrosine phosphatase expressed primarily in hematopoietic and epithelial cells and has been shown to dephosphorylate a wide spectrum of phosphoproteins involved in cell signaling of the receptors of the tyrosine kinase family. SHP-1 knockout mice are markedly glucose tolerant and insulin sensitive compared with wild-type controls. Dubois et al. (13) showed that these observations are a result of the enhanced insulin signaling through the IR substrate 1/2 (IRS1/2)/PI3K/Akt axis in the liver. Our group reported that in the kidney, elevated SHP-1 expression levels in mouse and human podocytes exposed to high-glucose (HG) concentrations result in reduced insulin and nephrin actions and podocyte dysfunction (14,15).

Current efforts have focused on the implication of epigenetic modifications as a potential mechanism underlying glycemic memory effects (16). Patients with albuminuria and microalbuminuria have shown higher levels of global DNA methylation than control subjects (17). More specifically in DN, Natarajan's group (18) showed that the activation mark H3K9/14ac, generally associated with transcriptionally active genome regions, is increased, whereas H3K9me2, H3K9me3, and H4K27me3, which are associated with repressed regions, are decreased in diabetic rodents. With consideration of the hyperglycemic memory effect as the major obstacle for optimal prevention and treatment of DN, we hypothesized that epigenetic changes cause persistent SHP-1 expression after glycemic control, resulting in sustained insulin signaling inhibition and DN progression.

RESEARCH DESIGN AND METHODS

Reagents and Antibodies

Primary antibodies for immunoblotting and immunochemistry were obtained from commercial sources, including actin (horseradish peroxidase; I-19), SHP-1 (C-19), SHP-1 (D11; immunofluorescence), IR-β (C-19), phosphotyrosine (PY99), phosphatase and tensin homolog (PTEN; C-20-R), transforming growth factor-β (TGF-β; SC-146), protein kinase C-δ (PKC-δ; C-20), cadherin (C-19), WT-1 (C-19), and rabbit and mouse peroxidase-conjugated secondary antibody from Santa Cruz Biotechnology; protein kinase B (Akt), extracellular signal-regulated kinase (ERK), phospho-Akt (D9E), and phospho-ERK (D13.14.4E) from Cell Signaling; purified monoclonal antibody against PTP1B (610139) and SHP-2 (610621) from BD Biosciences; monoclonal antibody against IR-β (AB69508) from Abcam; nephrin GP-N2 from PROGEN Biotechnik; podocin (P-0372) from Sigma; collagen type IV from Novus Biological; Alexa Fluor 546–conjugated anti-rabbit and Alexa Fluor 488–conjugated anti-guinea pig from Jackson ImmunoResearch; and Alexa Fluor 594–conjugated anti-mouse from Invitrogen. All other reagents used, including RPMI medium, EDTA, leupeptin, phenylmethylsulfonyl fluoride, aprotinin, insulin, D-glucose, D-mannitol, fluorescein isothiocyanate-inulin, sodium orthovanadate, and actinomycin D, were purchased from Sigma-Aldrich; FBS and penicillin-streptomycin were obtained from Invitrogen.

Animals and Experimental Design

C57BL/6J (*Ins2*$^{+/+}$) and diabetic heterozygous male *Ins2*$^{+/C96Y}$ (Akita) mice were purchased from The Jackson Laboratory and bred in our animal facility. Throughout the study period, animals were provided with free access to water and standard rodent chow (Harlan Teklad). All experiments were conducted in accordance with the Canadian Council of Animal Care and Institutional Guidelines and were approved by the Animal Care and Use Committees of the University of Sherbrooke according to National Institutes of Health guidelines. After 4 months of uncontrolled diabetes, animals received two insulin implants (Linbit; LinShin Canada) subcutaneously per month to normalize blood glucose levels, and these implants were replaced every month over a 2-month period (*Ins2*$^{+/C96Y}$ + ins). Blood glucose levels and animal weight were recorded every week.

Blood Glucose, Insulin Levels, Urinary Albumin Excretion, and Glomerular Filtration Rate Measurements

Blood glucose was measured by a glucometer (Contour; Bayer). Twenty-four–hour urine collections were obtained from mice 1 day before death by housing them in individual mouse metabolic cages (Nalgene Nunc International) with free access to water and rodent mash. Urinary creatinine concentration was measured using alkaline picrate colorimetry based on Jaffe reaction (The Creatinine Companion; Exocell), and albumin levels were measured by using an indirect competitive ELISA according to the manufacturer's instructions (Albuwell M; Exocell). The glomerular filtration rate (GFR) was evaluated by using fluorescein isothiocyanate-inulin clearance as described previously (19).

Histopathology and Transmission Electron Microscopy

Right mouse kidneys were harvested for pathology examination, and sections were fixed in 4% paraformaldehyde (Sigma-Aldrich) and then transferred to 70% ethanol for immunohistochemistry. The tissue was embedded in paraffin, and 4-μm sections were stained with periodic acid Schiff stain and hematoxylin-eosin (Sigma-Aldrich). Left mouse kidneys were used for transmission and scanning electron microscopy to evaluate podocyte structure and foot process effacement as previously described (14).

Immunohistochemistry

Immunohistochemistry of kidney sections was performed with the ABC Kit from Vector Laboratories according to the manufacturer's protocol. Coloration was obtained by incubating sections in 3,3′-diaminobenzidine solution

(Vector Laboratories). Counterstaining of the nucleus was done using Gill's Hematoxylin (Vector Laboratories).

Mesangium Expansion, Glomerular Hypertrophy, and Quantitation of Podocyte Cell Death

Mesangial matrix expansion and glomerular hypertrophy were evaluated quantitatively as previously described (14). Apoptotic nuclei of kidney sections were detected using the TACS 2 Tdt-Fluor In Situ Apoptosis Detection Kit (Trevigen) according to the manufacturer's instructions as previously described (14). Apoptotic podocytes were counted when both podocyte markers and Tdt-fluorescein–positive cells colocalized on all glomeruli (20–30) on the transverse section of the left kidney.

Immunofluorescence

Kidneys from *Ins2*$^{+/+}$, *Ins2*$^{+/C96Y}$, and *Ins2*$^{+/C96Y}$ mice treated with insulin implants were frozen in optimal cutting temperature compound (BDH Chemicals) embedding resin in cryomolds on a block of dry ice and sectioned at 8 μm (Leica cryostat). Immunofluorescence of the sections using nephrin, podocin (1:200), phospho-Akt, and SHP-1 antibodies were performed as previously described (14). Sections were examined with a Plan Apochromat 60× oil immersion objective (numerical aperture 1.42) mounted on an inverted spectral scanning confocal microscope (FV1000; Olympus, Tokyo, Japan) as previously described (15). Images of one experiment were taken at the same time under identical settings and handled similarly in Adobe Photoshop across all images.

Systemic Injection of Insulin

The insulin signaling pathway was evaluated by injecting insulin 5 mU/g i.v. in *Ins2*$^{+/+}$, *Ins2*$^{+/C96Y}$, and *Ins2*$^{+/C96Y}$ mice treated with insulin implants. The right kidney was removed before insulin injection and served as an internal control (nonstimulated). Fifteen minutes after the insulin injection, the left kidney was removed for protein extraction.

Cell Culture and Adenoviral Vector Transfection

The mouse podocyte cell line was used and cultured as previously described (14,20). After differentiation of podocytes, the medium was changed to RPMI 0.1% FBS containing normal glucose (NG) (5.6 mmol/L + 19.4 mmol/L mannitol to adjust osmotic pressure) or HG (25 mmol/L) up to 120 h. To mimic the reversibility phenomenon, podocytes were exposed to HG for 96 h and then NG for the last 24 h (HG + NG). Adenoviral vectors containing green fluorescent protein (Ad-GFP) and dominant-negative SHP-1 (Ad-dnSHP-1) were used to infect podocytes as reported previously (14).

Immunoprecipitation and Immunoblot Analyses

Immunoprecipitation assays were performed as described previously (14). For immunoblot analysis, 10–50 μg of lysate proteins were separated by SDS-PAGE and then transferred to a polyvinylidene fluoride membrane, which was blocked with 5% skim milk. Proteins were identified by enhanced chemiluminescence (Pierce Thermo Fisher Scientific).

Real-Time PCR Analyses

Real-time PCR was performed to evaluate mRNA expression of SHP-1, SHP-2, PTP1B, PKC-δ, IRS-1, IRS-2, IR-β, collagen type IV, TGF-β, and fibronectin as previously described (14). PCR primers are listed in Supplementary Table 1. GAPDH mRNA expression was used for normalization.

Caspase-3/7 Assay

Caspase-3 and -7 enzymatic activities were determined by quantification of cleaved substrate using luminescent assay Caspase-Glo 3/7 (Promega) as previously described (14).

Phosphatase Assay

We assessed phosphatase activity of SHP-1 by using a tyrosine phosphatase assay system (V2471; Promega) according to the manufacturer's instructions. SHP-1 was immunoprecipitated from cell lysates with a polyclonal antibody (C-19) prebound to Protein A Sepharose beads. The phosphatase activity was determined using the Infinite 200 PRO NanoQuant (Tecan Group).

Isolation of the Glomeruli

Renal cortexes of three kidneys (one per mouse) were combined and minced, and all tissue was passed through a 200-μm, 150-μm, and 75-μm sieve. The glomeruli that remained at the top of 75-μm sieve were collected with PBS and centrifuge for 10 min at 500*g*. The glomeruli samples (three kidneys per sample, four samples per group) were then used for chromatin immunoprecipitation (ChIP) assay.

ChIP Assay

At the end of each treatment, ChIP assays were performed as described by Kuo and Allis (21), with minor modifications as previously described (22). At the end of treatment, podocytes or glomeruli were cross-linked by adding formaldehyde 1.1% for 15 min at room temperature and glycine 1 mol/L for the last 5 min. Cells and glomeruli were then washed two times in PBS, and the pellet was resuspended in 200 μL of ChIP lysis buffer (1% SDS, 10 mmol/L EDTA, 50 mmol/L Tris-HCl [pH 8.0], and protease inhibitors) and sonicated with a Branson Sonifier 450 (Danbury, CT) at power setting 2 with 10-s pulses at duty cycle 90 (to obtain fragments <500 base pairs). The chromatin solution was diluted 10-fold in ChIP dilution buffer (0.01% SDS, 1.1% Triton X-100, 1.2 mmol/L EDTA, 16.7 mmol/L Tris [pH 8.1], 16.7 mmol/L NaCl, and protease inhibitors). One-tenth of the lysate was used for purification of total DNA. Each sample was precleared by incubating with 80 μL salmon sperm DNA/protein A-agarose 50% gel slurry (Upstate Biotechnology, Lake Placid, NY) for 30 min at 4°C. An aliquot of 5 μg of H3K4me1, H3K4me3, or H3K4ac (Abcam) were added and immunoprecipitated at 4°C overnight. The immunoprecipitate was collected using salmon sperm DNA/protein A-agarose and washed once with the following buffers in sequence: low-salt wash buffer (0.1% SDS, 1% Triton X-100, 2 mmol/L EDTA, 20 mmol/L Tris-HCl [pH 8.1], 150 mmol/L NaCl), high-salt wash buffer (0.1% SDS, 1%

Triton X-100, 2 mmol/L EDTA, 20 mmol/L Tris-HCl [pH 8.1], 500 mmol/L NaCl); LiCl wash buffer (0.25 mol/L LiCl, 1% IGEPAL CA-630, 1% sodium deoxycholate, 1 mmol/L EDTA, 10 mmol/L Tris-HCl [pH 8.1]); and TE buffer (10 mmol/L Tris-HCl [pH 8.0], 1 mmol/L EDTA). Beads were incubated with 1% SDS/0.1 mol/L $NaHCO_3$ solution for 30 min at 65°C to isolate the DNA. DNA-histone cross-links were reversed by incubation at 65°C overnight followed by proteinase K treatment. DNA was recovered by purification with the QIAquick PCR Purification Kit (QIAGEN). Immunoprecipitated DNA was measured by quantitative PCR. Total DNA was used as reference (input). Primers for the open reading frame of the gene were used as shown in Supplementary Fig. 3 as a control to demonstrate specificity of amplification of DNA associated with immunoprecipitated chromatin.

Statistical Analyses

Data are presented as mean ± SD for each group. Statistical analysis was performed by unpaired *t* test or by one-way ANOVA followed by Tukey test correction for multiple comparisons. Data in each group were checked for normal distribution using D'Agostino and Pearson normality test based on $\alpha = 0.05$. All results were considered statistically significant at $P < 0.05$.

RESULTS

Persistent Glomerular Dysfunction and Pathology in Type 1 Diabetic Akita Mice (*Ins2*$^{+/C96Y}$) Treated With Insulin Implants

We and others have previously shown that the genetically modified type 1 diabetic model (*Ins2*$^{+/C96Y}$) exhibited renal dysfunction (elevated urine albumin-to-creatinine

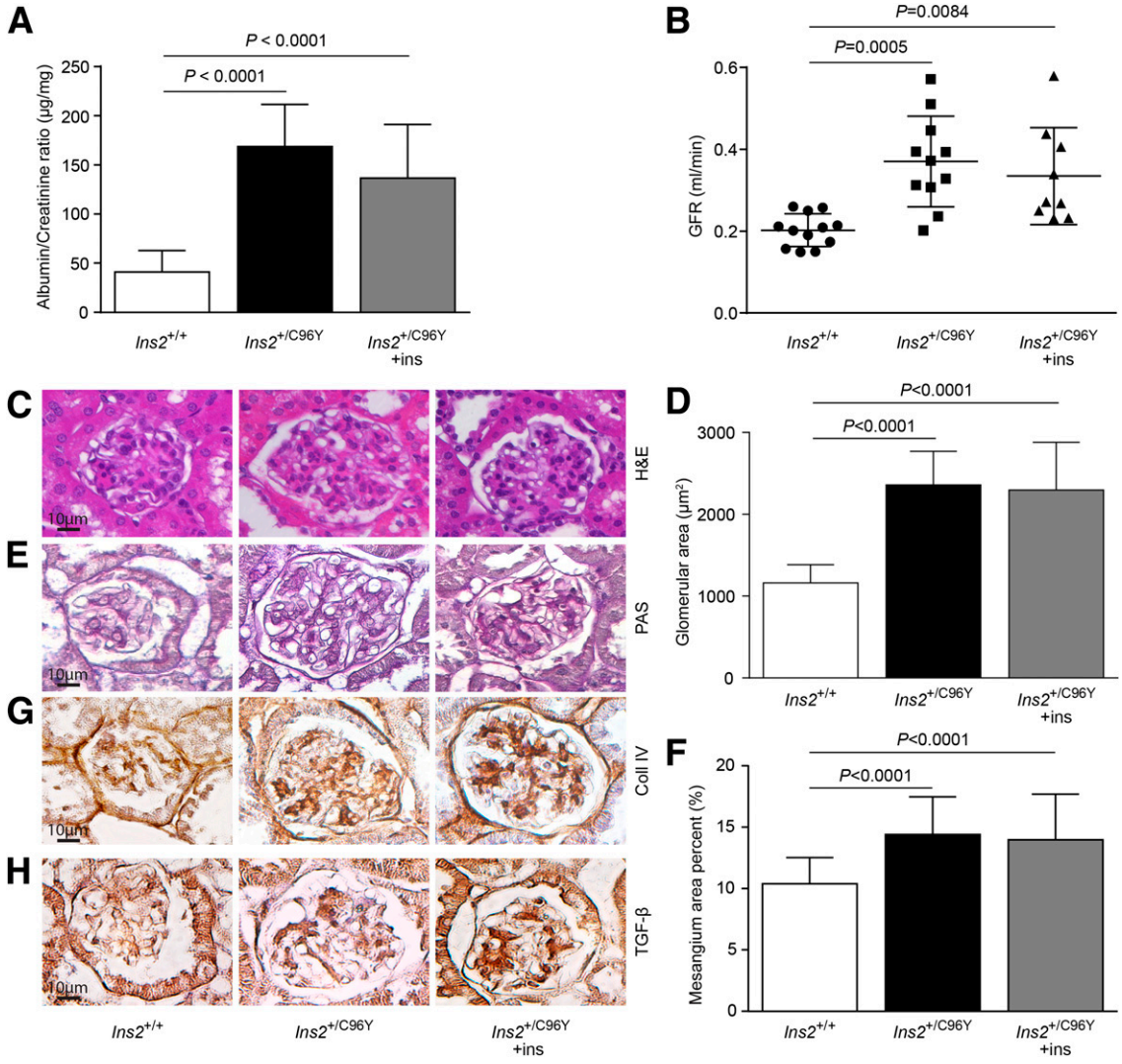

Figure 1—Persistence of renal dysfunction and glomerular histopathology in *Ins2*$^{+/C96Y}$ mice treated with insulin implants. Albumin-to-creatinine ratio (*A*) and GFR (*B*) were measured at 7 months of age in renal glomeruli of *Ins2*$^{+/+}$, *Ins2*$^{+/C96Y}$, and *Ins2*$^{+/C96Y}$ + ins mice at 5 months of age. Renal cross-sections were stained with hematoxylin-eosin (H&E) (*C*) and periodic acid Schiff (PAS) (*E*) and for collagen type IV (Coll IV) (*G*) and TGF-β (*H*) expression. Glomerular hypertrophy (*D*) and mesangium expansion (*F*) were quantified. Data are mean ± SD of three to four glomeruli of 11 mice per group.

ratio and GFR) and pathology (glomerular hypertrophy and mesangial cell expansion) compared with control littermates (14,23). As expected, diabetic *Ins2*$^{+/C96Y}$ mice exhibited an elevated urine albumin-to-creatinine ratio by 3.3-fold ($P < 0.0001$) and GFR (0.206 vs. 0.395 mL/min, $P < 0.0001$) compared with nondiabetic *Ins2*$^{+/+}$ mice (Fig. 1*A* and *B*). To evaluate the hyperglycemic memory phenomenon, diabetic mice were treated

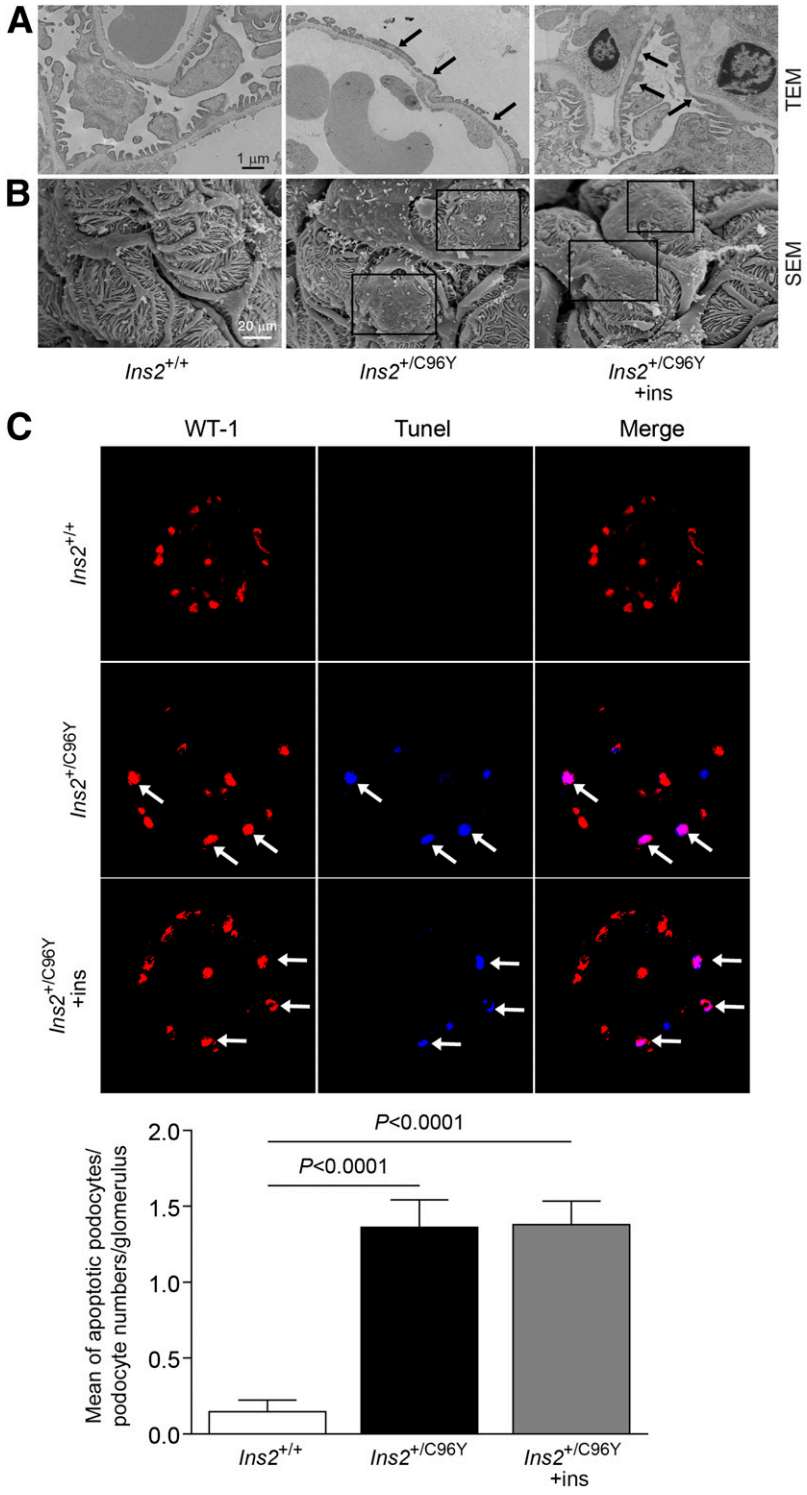

Figure 2— Foot process effacement and podocyte cell death. Transmission electron microscopy (TEM) (*A*) and scanning electron microscopy (SEM) (*B*) of podocyte foot process effacement (arrows and boxes). *C*: Immunofluorescence of podocytes (WT-1; red) and apoptosis-positive cells (TUNEL; blue) in the glomerulus of *Ins2*$^{+/+}$, *Ins2*$^{+/C96Y}$, and *Ins2*$^{+/C96Y}$ + ins mice at 5 months of age. Arrows represent colocalization of podocyte and apoptotic markers. Data are mean ± SD of three to four glomeruli of 10 mice per group.

with insulin implants for 2 months. Mice in the interventional glycemic group gained weight and normalized glucose levels during these last 2 months (Supplementary Table 2). Of note, despite euglycemia for the last 2 months, albuminuria and GFR remained significantly higher in the diabetic mice treated with insulin implants compared with nondiabetic counterparts, suggesting that renal dysfunction persisted despite glucose normalization for 2 months after uncontrolled hyperglycemia for 4 months. Diabetic *Ins2*$^{+/C96Y}$ mice demonstrated glomerular hypertrophy ($P < 0.0001$) (Fig. 1*C* and *D*) and expansion of the mesangium ($P < 0.0001$) (Fig. 1*E* and *F*) as well as increased collagen type IV– and TGF-β–positive staining compared with nondiabetic mice (Fig. 1*G* and *H*). Similarly, blinded assessment of glomerular hypertrophy ($P < 0.0001$), mesangium expansion ($P < 0.0001$), and collagen type IV and TGF-β expression remained elevated despite systemic glucose normalization with insulin implants for the last 2 months in diabetic mice (Fig. 1*C*–*H*).

Foot Process Effacement, Podocyte Loss, and Markers of Glomerular Injury

Podocyte effacement and cell death are early markers of glomerular dysfunction in DN. Both transmission (Fig. 2*A*) and scanning (Fig. 2*B*) electron microscopy showed podocyte effacement (arrows and boxes) in diabetic *Ins2*$^{+/C96Y}$ mice as well as in diabetic mice treated with insulin implants. Immunofluorescence analyses were performed to evaluate podocyte death. Increased positive apoptotic signal (TUNEL) in podocytes (WT-1 staining) was observed in diabetic *Ins2*$^{+/C96Y}$ mice compared with nondiabetic *Ins2*$^{+/+}$ mice. Podocyte loss was also detected in diabetic mice treated with insulin implants for the last 2 months after 4 months of uncontrolled hyperglycemia. Quantitative PCR analysis demonstrated that mRNA expression of collagen type IV, TGF-β, and fibronectin, recognized markers of glomerular injury, were significantly increased in diabetic *Ins2*$^{+/C96Y}$ mice compared with nondiabetic counterparts, and the normalized systemic glucose levels for the last 2 months with insulin implants did not reduce their expression (Fig. 3*A*–*C*).

Persistent Insulin Unresponsiveness in the Renal Cortex of Diabetic Mice

To evaluate whether the inhibition of insulin actions persisted in the diabetic intervention group, insulin 5 mU/g i.v. was injected in all groups of mice. The right kidney was removed before the insulin injection and served as the internal control (nonstimulated). Fifteen minutes after the injection, insulin-stimulated Akt and ERK phosphorylation was significantly blunted in the renal cortex (Fig. 4*A*) and podocytes (using podocin as a podocyte marker) (Fig. 4*B*) of both nontreated and insulin implant–treated diabetic mice compared with *Ins2*$^{+/+}$ mice. The inhibition of the insulin signaling pathway in diabetes was not due to any change in the expression of IR-β, IRS1, or IRS2 (Fig. 4*C*–*E*).

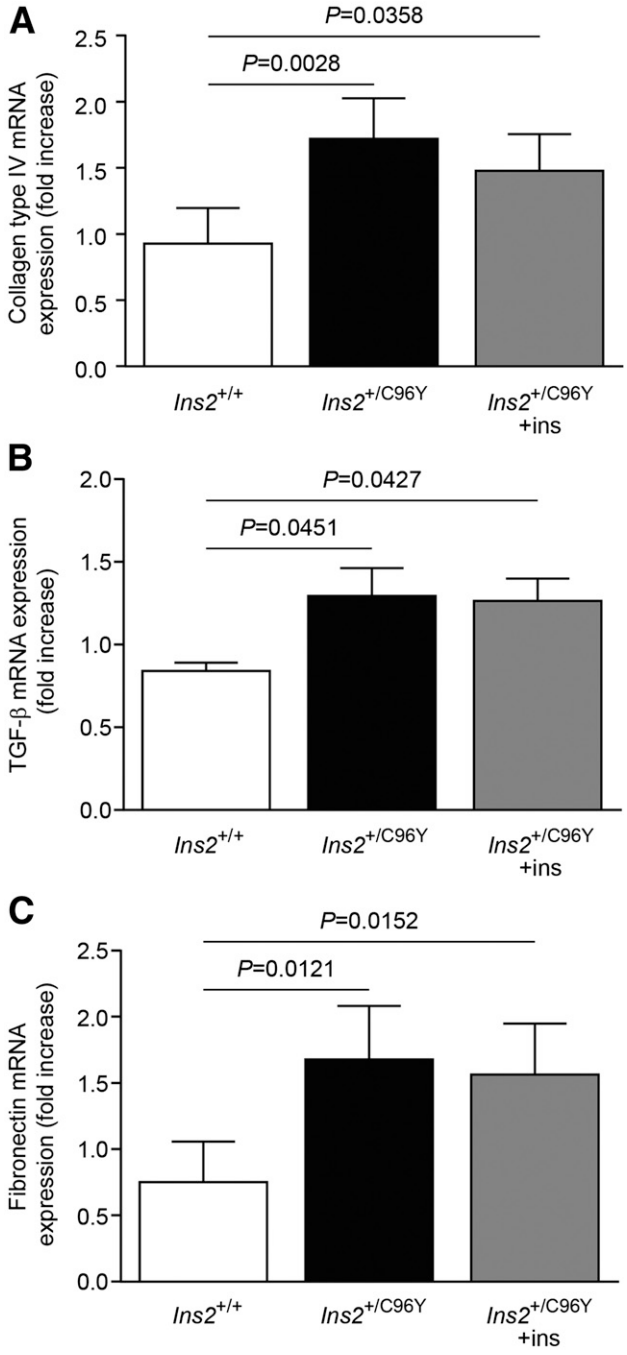

Figure 3—Sustained expression levels of renal markers of DN. Expression of collagen type IV (*A*), TGF-β (*B*), and fibronectin (*C*) mRNA levels in the renal cortex of *Ins2*$^{+/+}$, *Ins2*$^{+/C96Y}$, and *Ins2*$^{+/C96Y}$ + ins mice at 5 months of age. Data are mean ± SD of six to eight mice per group.

SHP-1 Expression Remained Elevated in Podocytes of Diabetic Mice Treated With Insulin Implants

Elevated SHP-1 expression has been previously reported in retinal and renal cortex using two different mouse models of type 1 diabetes (14,24,25). As expected, SHP-1 mRNA and protein expression were elevated in the renal cortex of *Ins2*$^{+/C96Y}$ mice. Despite systemic euglycemia

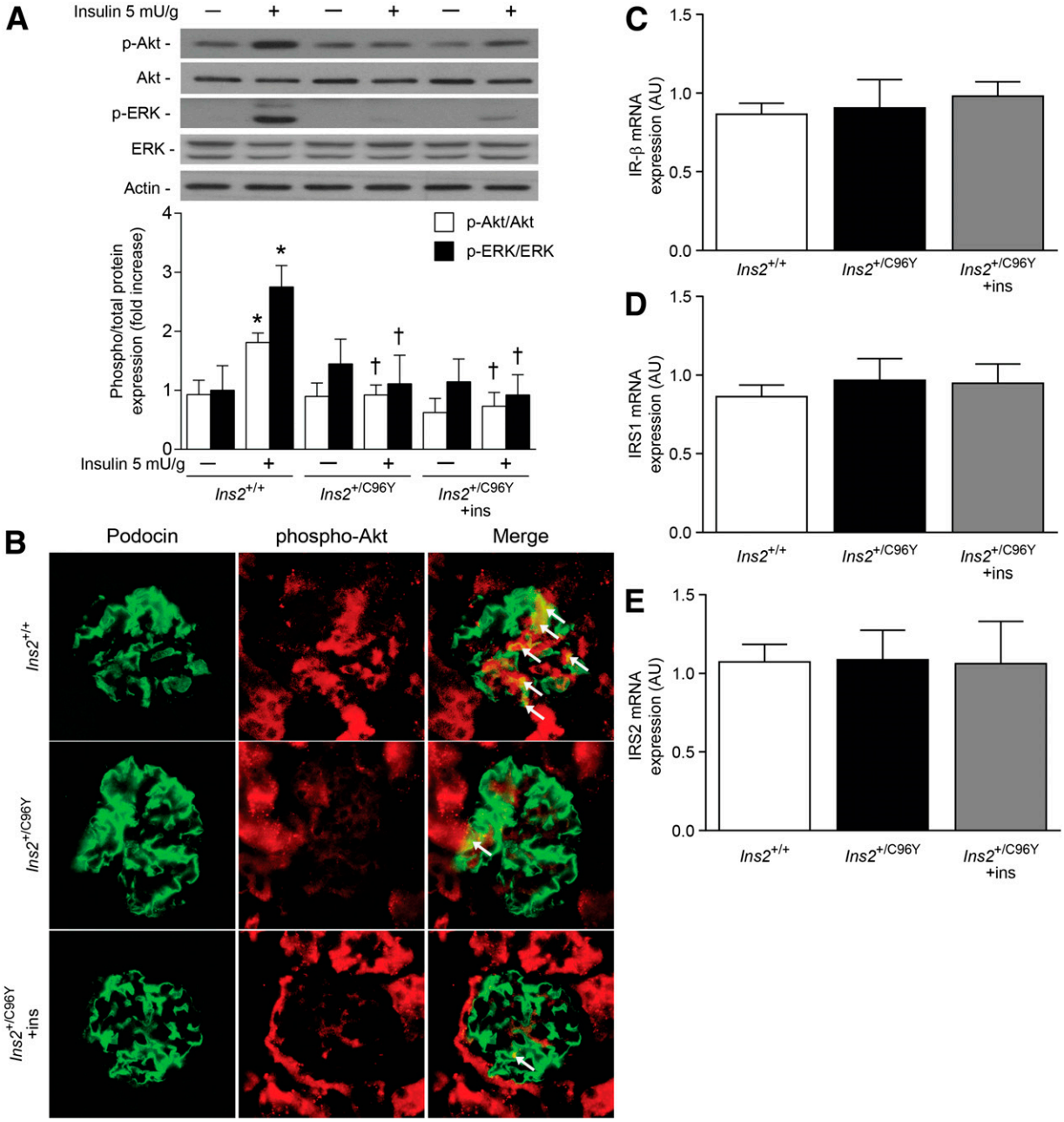

Figure 4—Persistence of insulin signaling inhibition in *Ins2*$^{+/C96Y}$ mice treated with insulin implants. Insulin was injected intravenously for 15 min at 7 months of age in *Ins2*$^{+/+}$, *Ins2*$^{+/C96Y}$, and *Ins2*$^{+/C96Y}$ + ins mice at 5 months of age. *A*: Expression of phospho (p)-Akt, Akt, phospho-ERK, ERK, and actin were detected by immunoblot and densitometry quantitation. *B*: Immunofluorescence labeling of podocytes (podocin; green) and phospho-Akt (red). Arrows represent colocalization of podocin and phospho-Akt. IR-β (*C*), IRS1 (*D*), and IRS2 (*E*) mRNA expression were evaluated. Data are mean ± SD of five to six independent experiments. **P* < 0.05 vs. unstimulated *Ins2*$^{+/+}$ mice; †*P* < 0.05 vs. insulin-stimulated *Ins2*$^{+/+}$ mice. AU, arbitrary units.

with insulin implants for the last 2 months, SHP-1 expression remained elevated in diabetic mice (Fig. 5*A* and *B*). We have shown that SHP-2 and PTP1B, other protein phosphatases that have been implicated in the insulin signaling pathway, were unchanged in renal cortex of diabetic mice and remained unaffected by treatment with insulin implants (Fig. 5*A* and *B*). Furthermore, with use of immunofluorescence analysis of nephrin, a podocyte-specific marker, we confirmed that the increase of SHP-1 expression continued to be elevated in podocytes of diabetic *Ins2*$^{+/C96Y}$ mice treated with insulin implants (Fig. 5*C*).

Persistent SHP-1 Expression Correlated With Podocyte Loss Despite Glucose Normalization

Caspase-3/7 enzymatic activity, a marker of cell death, was measured in podocytes cultured in 5.6 mmol/L (NG) or 25 mmol/L (HG) glucose concentrations for up to 120 h. To replicate the hyperglycemic memory phenomenon, podocytes were exposed to HG for 96 h before returning

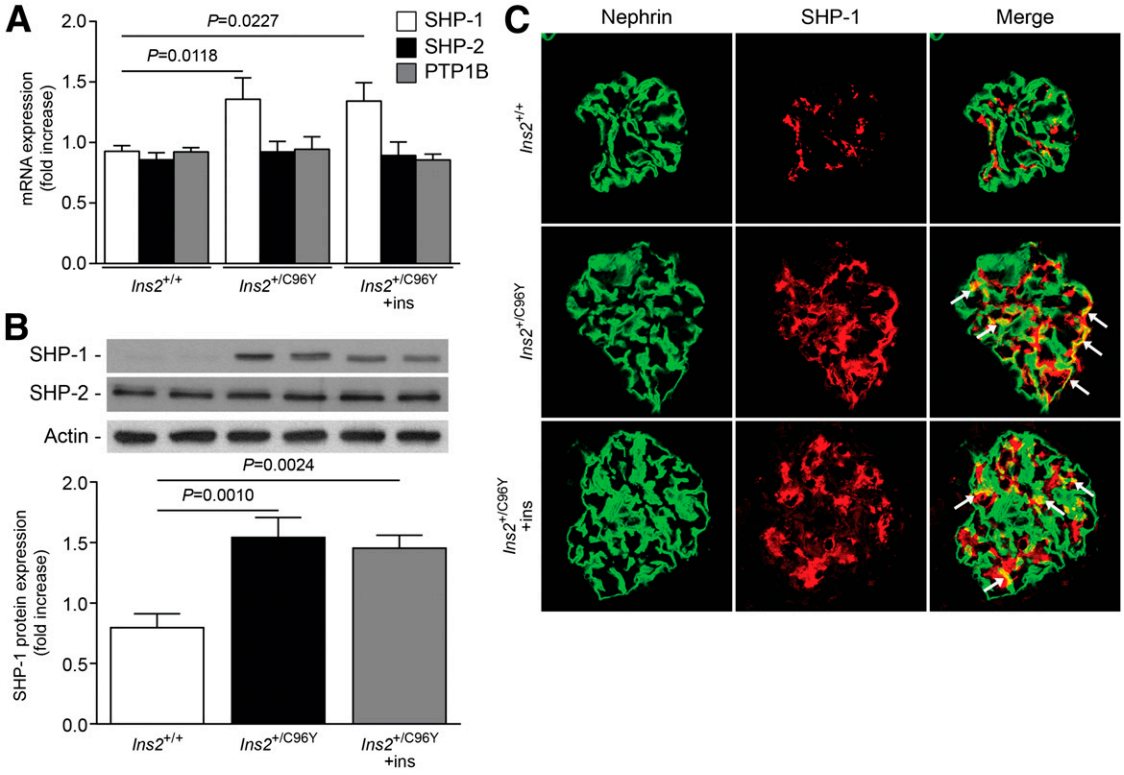

Figure 5—Expression of SHP-1 remained elevated despite glucose level restoration in renal glomeruli of *Ins2*$^{+/C96Y}$ mice. SHP-1, SHP-2, and PTP1B mRNA (*A*) and protein (*B*) expression from the renal cortex at 7 months of age in *Ins2*$^{+/+}$, *Ins2*$^{+/C96Y}$, and *Ins2*$^{+/C96Y}$ + ins mice at 5 months of age. *C*: Immunofluorescence labeling of podocytes (nephrin; green) and SHP-1 (red). Arrows represent colocalization of nephrin and SHP-1. Protein expression was detected by immunoblot and densitometry quantitation. Data are mean ± SD of five to six independent experiments.

glucose levels to 5.6 mmol/L (HG + NG). Exposing podocytes to HG levels for 120 h increased caspase-3/7 enzymatic activity by 32% (P = 0.0312) (Fig. 6*A*). Podocytes exposed to 96 h of HG and NG levels for the last 24 h showed similar caspase-3/7 enzymatic activity compared with 120 h of HG exposure, suggesting that the apoptotic signal continued to be active despite returning glucose concentration to a normal range. A longer period in NG after the HG treatment produced similar results. Of note, adding 10 nmol/L insulin for the last 24 h did not prevent HG effects on podocyte caspase-3/7 activity even when the 24-h insulin treatment was done in NG after the HG exposure (HG + NG) (Fig. 6*A*). These data suggest that HG-induced insulin unresponsiveness is not easily reversed.

To follow with our findings that podocyte cell death induced by HG concentrations was associated with increased SHP-1 expression (14), we evaluated whether the persistent caspase-3/7 enzymatic activity in podocytes exposed to NG after being cultured in HG concentrations displayed elevated SHP-1 expression. The data demonstrate that mRNA and protein expression as well as phosphatase activity of SHP-1 were significantly increased in cultured podocytes exposed to HG concentrations (Fig. 6*B–D*). No change was observed in the expression of SHP-2 and PTP1B. Similar to in vivo data, the mRNA and protein expression of SHP-1 as well as its phosphatase activity remained elevated despite returning podocytes to NG levels for 24 h (Fig. 6*B–D*) and 48 h (Supplementary Fig. 1*A* and *B*) after HG exposure. Importantly, the half-life of SHP-1 mRNA by treating podocytes with actinomycin D 5 mg/mL was similar in NG and HG conditions, suggesting that persistent expression of SHP-1 is not due to abnormal degradation or decay of SHP-1 in HG conditions (data not shown).

Sustained Podocyte Unresponsiveness to Insulin Stimulation Is Caused by SHP-1

We previously reported that the increased expression SHP-1 was associated with the incapacity of insulin to induce Akt phosphorylation (14). The current results indicate that the persistent increased expression and activity of SHP-1 in podocytes reduced the capacity of insulin to phosphorylate its receptor (IR-β) and subsequently Akt (Fig. 7*A*). To demonstrate the continuous inhibition of IR activity, podocytes were infected with Ad-dnSHP-1. In podocytes overexpressing Ad-GFP, insulin-induced phosphorylation of IR-β was completely blunted during HG exposure. In contrast, the overexpression of Ad-dnSHP-1 rescued insulin action of IR-β phosphorylation (Fig. 7*B*).

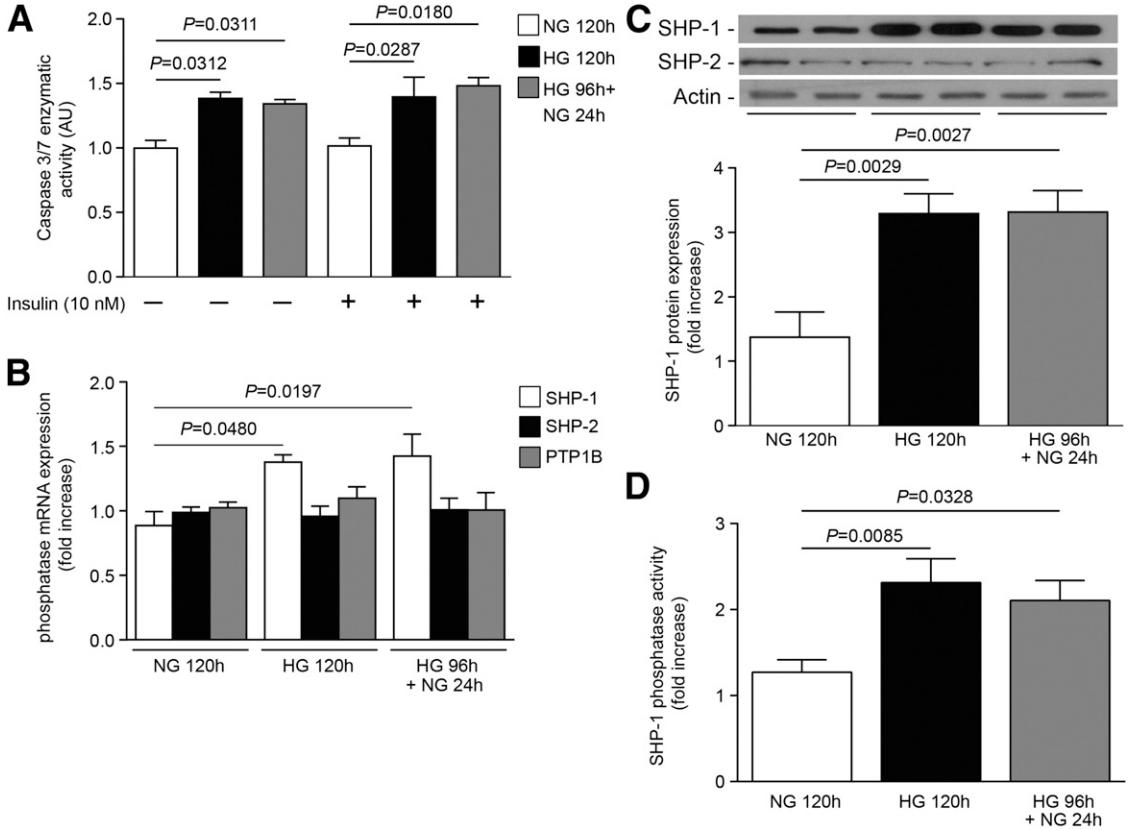

Figure 6—HG levels induce persistent caspase-3/7 activity, SHP-1 expression, and phosphatase activity. Podocytes were incubated with NG (5.6 mmol/L + 19.4 mmol/L mannitol) and HG (25 mmol/L) for 120 h or HG for 96 h and then in NG for an additional 24 h (HG + NG) in the absence or presence of insulin during the last 24 h. *A*: Caspase-3/7 enzymatic activity was measured according to the manufacturer's instructions. SHP-1, SHP-2, and PTP1B mRNA (*B*) and protein (*C*) expression were measured by quantitative PCR and immunoblot analyses. *D*: SHP-1 phosphatase activity was measured according to the manufacturer's instructions. Data are mean ± SEM of four independent experiments. AU, arbitrary units.

HG Exposure Caused Increased Acetylation and Monomethylation of Histone H3 at the SHP-1 Promoter

The data demonstrate both in vivo and in vitro that SHP-1 was persistently expressed in type 1 diabetic mouse glomeruli and podocytes exposed to HG despite glucose level normalization. Our group has previously demonstrated that PKC-δ activation by HG levels is responsible for the increase expression of SHP-1 in podocytes (25). However, although PKC-δ activity was elevated, there was no significant change of PKC-δ mRNA and protein expression in podocytes exposed to HG (Supplementary Fig. 2). Thus, epigenetic regulation, such as histone modifications, could be an explanation for the persistent SHP-1 expression. Therefore, we performed ChIP assays of the SHP-1 promoter region with antibodies against histone 3 (H3) acetylation, monomethylation (me1), and trimethylation (me3). The data show that the promoter region of the SHP-1 gene was enriched with H3K9/14/27ac and H3K4me1 (Fig. 8*A* and *B*), whereas no change was observed in H3K4me3 (Fig. 8*C*). Moreover, we evaluated whether H3K9/14 and H3K4me1 enrichment in cultured podocytes occurred in vivo. Isolation of glomeruli from each group of mice demonstrated that H3K9/14ac and H3K4me1 marks were enhanced in diabetic glomeruli and remained elevated in glomeruli of diabetic mice treated with insulin implants (Fig. 8*D* and *E*). These data strongly support the notion that persistent expression of SHP-1 causing permanent insulin inhibition and dysfunction in podocytes was triggered by epigenetic modifications at the SHP-1 promoter region.

DISCUSSION

The metabolic memory effect (or legacy effect) has received much interest since 2003, but the biological mechanisms of this glycemic memory phenomenon remain elusive. The metabolic memory effect is generally defined as a period of good metabolic control that results in a long-term beneficial effect on vascular end points. On the other hand, the metabolic changes caused by the persistence of hyperglycemic stress despite glucose normalization has been defined as the hyperglycemic memory phenomenon (26,27). This observation was initially reported in dogs, rats, and mice with alloxan- and streptozotocin-induced diabetes, where a poor glycemic period followed by a period of good control led to similar rates of retinopathy and expression of fibronectin mRNA in the kidney cortex (28–30). These experiments implied that

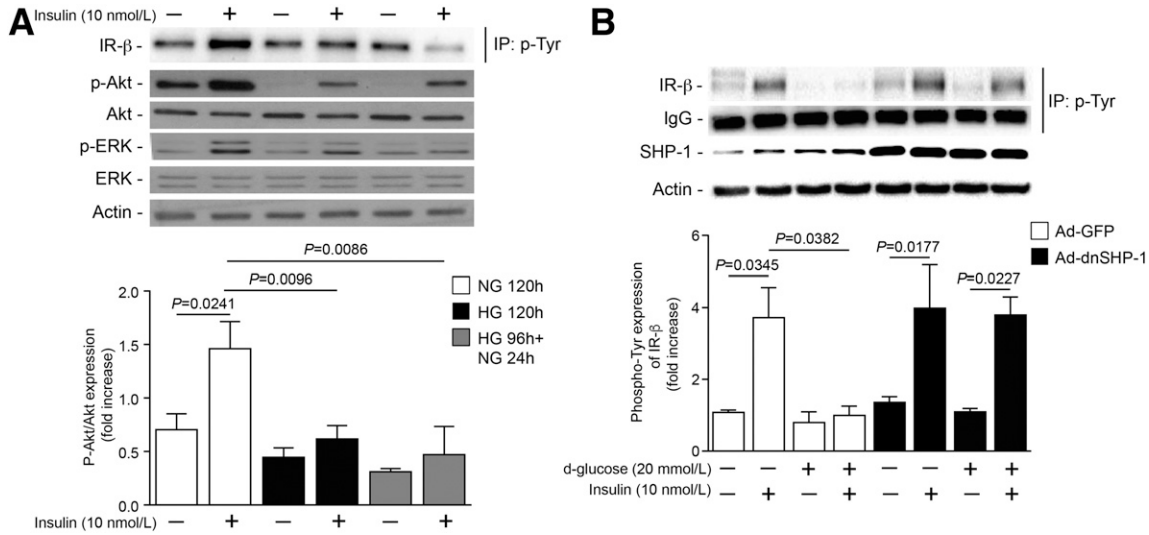

Figure 7—Continuous inhibition of the insulin-stimulated IR-β phosphorylation (p) in podocytes exposed to HG levels is regulated by SHP-1. *A*: Podocytes were incubated with NG (5.6 mmol/L + 19.4 mmol/L mannitol) and HG (25 mmol/L) for 120 h or HG for 96 h and then in NG for an additional 24 h (HG + NG) followed by insulin stimulation for 5 min. *B*: Podocytes were transfected with either Ad-GFP or Ad-dnSHP-1 before exposure to NG, HG, or HG + NG. Expression of phosphotyrosine (p-Tyr), phospho-Akt, Akt, phospho-ERK, ERK, and actin were detected by immunoblot and densitometry quantitation. Data are mean ± SEM of four independent experiments. IP, immunoprecipitation.

some irreversible biological changes could be implicated in the progression of microvascular complications after a prolonged period of hyperglycemia. Thus, a better understanding of the pathways leading to hyperglycemic memory may contribute to designing mechanism-driven strategies to blunt vascular damage in patients with diabetes to improve vascular outcomes. The current study provides strong evidence that SHP-1 is persistently activated and expressed in diabetic podocytes, causing sustained inhibition of insulin signaling and podocyte dysfunction and cell death. Furthermore, these data demonstrate that the persistent activation of SHP-1 can be explained by epigenetic changes at the SHP-1 promoter region, thus providing a potential explanation for the hyperglycemic memory effect in podocytes and progression of DN despite glucose level normalization.

Decreased podocyte number and podocyte foot process effacement have been shown to occur in patients with diabetes during the early phases of kidney damage (31), even before the onset of microalbuminuria and more-advanced DN (32). In addition, several clinical observations have suggested that disruption of normal insulin actions is a part of the etiology of DN. A previous study indicated through protein analysis that podocytes have the highest levels of both IR-β and IRS1 expression compared with other glomerular cells, such as renal endothelial and mesangial cells (33). Although the primary defect in type 1 diabetes is diminished insulin secretion, insulin resistance occurrence in type 1 diabetes is widely recognized (34,35), providing support for a renal insulin resistance in type 1 diabetes (11,36). Insulin resistance was shown to precede microalbuminuria in 16 patients with uncomplicated type 1 diabetes (37). Coward et al. (38) showed that podocytes are insulin-responsive cells. By using both a type 1 and a type 2 diabetic rat model, a study demonstrated that the insulin responses in renal endothelial cells were reduced in part by the hyperglycemia-induced polyubiquitination of IRS-1, whereas in the tubular compartment, the insulin signaling pathway was unaffected (33). However, the current study supports the notion that the insulin resistance phenomenon occurs in podocytes and is caused by hyperglycemia-induced persistent expression and activity of SHP-1, resulting in decreased IR-β phosphorylation. Moreover, loss of Akt2, specifically in podocytes, resulted in a rapid disease progression in a mouse model of glomerular diseases (39). Taken together, the capacity of insulin to stimulate Akt is important for podocyte function, and any disruption of its signaling will result in podocyte loss.

Several articles explored the possibility that epigenetic modifications induced by hyperglycemia explain the hyperglycemic memory phenomenon. Studies have demonstrated that HG exposure prompted long-lasting activation of epigenetic changes by promoting Set7 recruitment and H3K4me1 enrichment at the promoter region of the p65 subunit of the nuclear factor-κB in bovine aortic endothelial cells (40,41). In general, acetylation of lysine residues of histone (i.e., H3K9/14) at the gene promoters is associated with transcriptional activation. In contrast, lysine methylation can result in either repression or activation of gene transcription, depending on the amino acid residue modified and the degree of methylation. For example, mono- (me1), di- (me2), and trimethylation (me3) of H3K4 and H3K36 are associated with transcriptionally active genome regions, whereas methylation of H3K9 and H3K27 are associated with gene repression (42). Previous

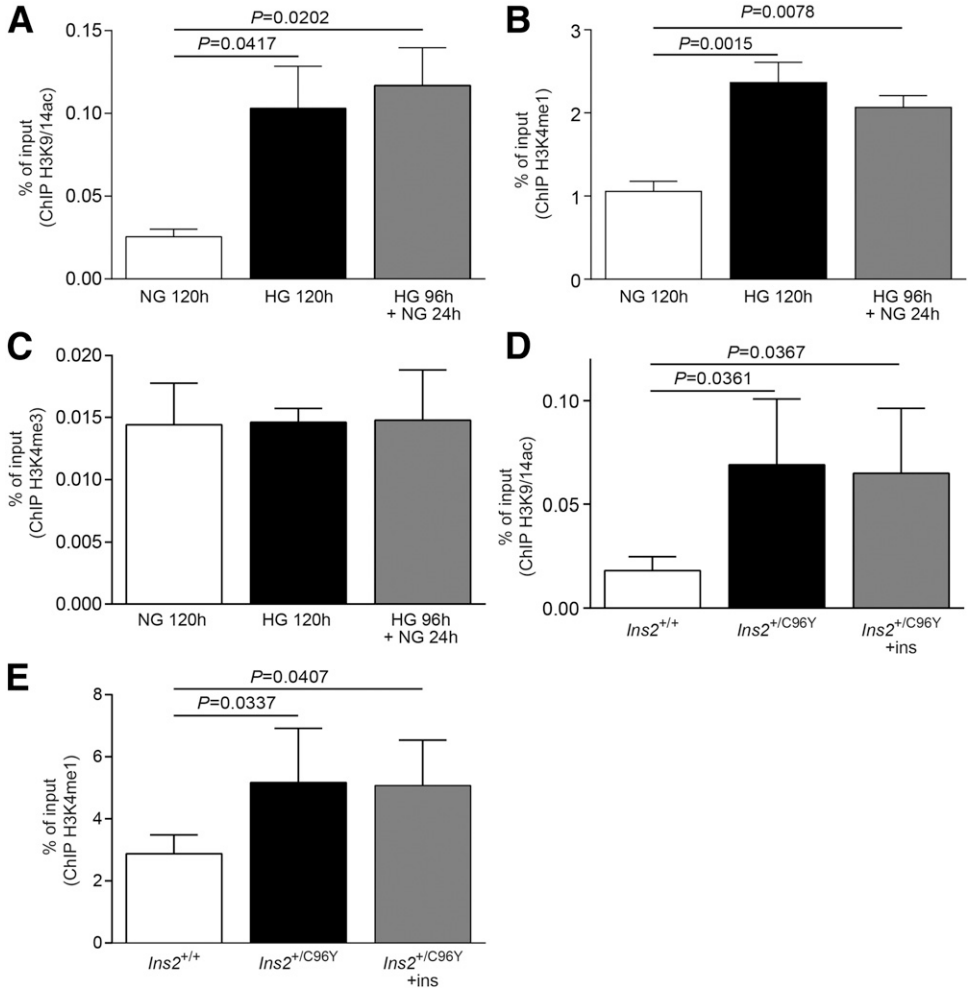

Figure 8— Epigenetic modifications of the SHP-1 promoter region caused persistent SHP-1 expression in renal podocytes exposed to HG levels. *A–C*: Podocytes were incubated with NG (5.6 mmol/L + 19.4 mmol/L mannitol) and HG (25 mmol/L) for 120 h or HG for 96 h and then in NG for an additional 24 h (HG + NG). *D* and *E*: Glomeruli of three kidneys (one per mouse) were isolated at 7 months of age from *Ins2*$^{+/+}$, *Ins2*$^{+/C96Y}$, and *Ins2*$^{+/C96Y}$ + ins mice at 5 months of age. ChIP assay using H3K9/14ac (*A* and *D*), H3K4me1 (*B* and *E*), and H3K4me3 (*C*) antibodies was performed, and ChIP-enriched DNA samples were analyzed by quantitative PCR using the primer of SHP-1 promoter. Data are mean ± SEM of four (in vivo; 12 mice per group) to five (in vitro) independent experiments.

studies have shown that TGF-β–induced collagen IV, connective tissue growth factor, and plasminogen activator inhibitor 1 expression is associated with activation of lysine marks in mesangial cells (43). Studies that used podocytes exposed to HG concentrations showed increased p66^{Shc} expression in an activated protein C–dependent manner that is accompanied by hyperacetylation of histone at the p66^{Shc} promoter (44). The current data demonstrate that HG exposure induced an enrichment of H3K4me1 and H3K9/14ac at the SHP-1 promoter region and that these epigenetic modifications were sustained despite glucose level normalization. These results may explain why elevated activity and expression levels of SHP-1 persisted in podocytes and renal glomeruli of diabetic mice. Another study reported that altered activity of Sirt1 and HADC4 have been implicated in the pathogenesis of diabetes-induced renal injury and DN (45,46), suggesting that other epigenetic modifications may contribute to the pathogenesis of DN.

In conclusion, this study provides new insight into the persistent activation and expression of SHP-1 in podocytes, causing sustained insulin resistance and podocyte dysfunction that may account for the observed hyperglycemic memory phenomenon responsible for the continued progression of diabetic renal complications. Because metabolic memory remains a major obstacle in the effective prevention and treatment of diabetic complications, targeting epigenetic changes of SHP-1 could be beneficial to halt the progression of renal injury.

Acknowledgments. The authors thank Anne Vezina (Department of Cell Anatomy, Université de Sherbrooke) for assistance with the histology services.

Funding. F.L. and B.D. are the recipients of a scholarship award from Fonds de Recherche du Québec–Santé. This work was supported by grants from the Canadian Institutes of Health Research (201209PNI, 201505MOP to P.G.), JDRF International (27-2012-531 to P.G), and Diabète Estrie. This work was performed at the Research Center of CHU de Sherbrooke and funded by Fonds de Recherche

du Québec–Santé. P.G. currently holds the Canadian Research Chair in Vascular Complications of Diabetes and is the recipient of a Scholarship Award from the Canadian Diabetes Association.

Duality of Interest. No potential conflicts of interest relevant to this article were reported.

Author Contributions. F.L., B.D., and P.G. contributed to the experiments, data analysis, and writing of the manuscript. A.G. contributed to the animal care and data research. N.G. contributed support and assistance with the ChIP assays. A.M.C. contributed to the data analysis and writing of the manuscript. P.G. is the guarantor of this work and, as such, had full access to all the data and takes responsibility for the integrity of the data and the accuracy of the data analysis.

References

1. Collins AJ, Kasiske B, Herzog C, et al. Excerpts from the United States Renal Data System 2006 annual data report. Am J Kidney Dis 2007;49(Suppl. 1):A6–A7, S1–S296

2. Writing Team for the Diabetes Control and Complications Trial/Epidemiology of Diabetes Interventions and Complications Research Group. Effect of intensive therapy on the microvascular complications of type 1 diabetes mellitus. JAMA 2002;287:2563–2569

3. Writing Team for the Diabetes Control and Complications Trial/Epidemiology of Diabetes Interventions and Complications Research Group. Sustained effect of intensive treatment of type 1 diabetes mellitus on development and progression of diabetic nephropathy: the Epidemiology of Diabetes Interventions and Complications (EDIC) study. JAMA 2003;290:2159–2167

4. de Boer IH; DCCT/EDIC Research Group. Kidney disease and related findings in the Diabetes Control and Complications Trial/Epidemiology of Diabetes Interventions and Complications study. Diabetes Care 2014;37:24–30

5. Cencioni C, Spallotta F, Greco S, Martelli F, Zeiher AM, Gaetano C. Epigenetic mechanisms of hyperglycemic memory. Int J Biochem Cell Biol 2014;51:155–158

6. Greka A, Mundel P. Cell biology and pathology of podocytes. Annu Rev Physiol 2012;74:299–323

7. Powell DW, Kenagy DN, Zheng S, et al. Associations between structural and functional changes to the kidney in diabetic humans and mice. Life Sci 2013;93:257–264

8. Meyer TW, Bennett PH, Nelson RG. Podocyte number predicts long-term urinary albumin excretion in Pima Indians with type II diabetes and microalbuminuria. Diabetologia 1999;42:1341–1344

9. Musso C, Javor E, Cochran E, Balow JE, Gorden P. Spectrum of renal diseases associated with extreme forms of insulin resistance. Clin J Am Soc Nephrol 2006;1:616–622

10. Thameem F, Puppala S, Schneider J, et al. The Gly(972)Arg variant of human IRS1 gene is associated with variation in glomerular filtration rate likely through impaired insulin receptor signaling. Diabetes 2012;61:2385–2393

11. Yip J, Mattock MB, Morocutti A, Sethi M, Trevisan R, Viberti G. Insulin resistance in insulin-dependent diabetic patients with microalbuminuria. Lancet 1993;342:883–887

12. Welsh GI, Hale LJ, Eremina V, et al. Insulin signaling to the glomerular podocyte is critical for normal kidney function. Cell Metab 2010;12:329–340

13. Dubois MJ, Bergeron S, Kim HJ, et al. The SHP-1 protein tyrosine phosphatase negatively modulates glucose homeostasis. Nat Med 2006;12:549–556

14. Drapeau N, Lizotte F, Denhez B, Guay A, Kennedy CR, Geraldes P. Expression of SHP-1 induced by hyperglycemia prevents insulin actions in podocytes. Am J Physiol Endocrinol Metab 2013;304:E1188–E1198

15. Denhez B, Lizotte F, Guimond MO, Jones N, Takano T, Geraldes P. Increased SHP-1 protein expression by high glucose levels reduces nephrin phosphorylation in podocytes. J Biol Chem 2015;290:350–358

16. Intine RV, Sarras MP Jr. Metabolic memory and chronic diabetes complications: potential role for epigenetic mechanisms. Curr Diab Rep 2012;12:551–559

17. Maghbooli Z, Larijani B, Emamgholipour S, Amini M, Keshtkar A, Pasalar P. Aberrant DNA methylation patterns in diabetic nephropathy. J Diabetes Metab Disord 2014;13:69

18. Reddy MA, Sumanth P, Lanting L, et al. Losartan reverses permissive epigenetic changes in renal glomeruli of diabetic db/db mice. Kidney Int 2014;85:362–373

19. Qi Z, Whitt I, Mehta A, et al. Serial determination of glomerular filtration rate in conscious mice using FITC-inulin clearance. Am J Physiol Renal Physiol 2004;286:F590–F596

20. Mundel P, Reiser J, Zúñiga Mejía Borja A, et al. Rearrangements of the cytoskeleton and cell contacts induce process formation during differentiation of conditionally immortalized mouse podocyte cell lines. Exp Cell Res 1997;236:248–258

21. Kuo MH, Allis CD. In vivo cross-linking and immunoprecipitation for studying dynamic protein:DNA associations in a chromatin environment. Methods 1999;19:425–433

22. Gévry NY, Lalli E, Sassone-Corsi P, Murphy BD. Regulation of Niemann-Pick c1 gene expression by the 3′5′-cyclic adenosine monophosphate pathway in steroidogenic cells. Mol Endocrinol 2003;17:704–715

23. Gurley SB, Mach CL, Stegbauer J, et al. Influence of genetic background on albuminuria and kidney injury in Ins2(+/C96Y) (Akita) mice. Am J Physiol Renal Physiol 2010;298:F788–F795

24. Geraldes P, Hiraoka-Yamamoto J, Matsumoto M, et al. Activation of PKC-delta and SHP-1 by hyperglycemia causes vascular cell apoptosis and diabetic retinopathy. Nat Med 2009;15:1298–1306

25. Mima A, Kitada M, Geraldes P, et al. Glomerular VEGF resistance induced by PKCδ/SHP-1 activation and contribution to diabetic nephropathy. FASEB J 2012;26:2963–2974

26. Pirola L, Balcerczyk A, Okabe J, El-Osta A. Epigenetic phenomena linked to diabetic complications. Nat Rev Endocrinol 2010;6:665–675

27. Ceriello A. Hypothesis: the "metabolic memory", the new challenge of diabetes. Diabetes Res Clin Pract 2009;86(Suppl. 1):S2–S6

28. Engerman RL, Kern TS. Progression of incipient diabetic retinopathy during good glycemic control. Diabetes 1987;36:808–812

29. Roy S, Sala R, Cagliero E, Lorenzi M. Overexpression of fibronectin induced by diabetes or high glucose: phenomenon with a memory. Proc Natl Acad Sci U S A 1990;87:404–408

30. Zhong Q, Kowluru RA. Epigenetic changes in mitochondrial superoxide dismutase in the retina and the development of diabetic retinopathy. Diabetes 2011;60:1304–1313

31. Jauregui A, Mintz DH, Mundel P, Fornoni A. Role of altered insulin signaling pathways in the pathogenesis of podocyte malfunction and microalbuminuria. Curr Opin Nephrol Hypertens 2009;18:539–545

32. Pagtalunan ME, Miller PL, Jumping-Eagle S, et al. Podocyte loss and progressive glomerular injury in type II diabetes. J Clin Invest 1997;99:342–348

33. Mima A, Ohshiro Y, Kitada M, et al. Glomerular-specific protein kinase C-β-induced insulin receptor substrate-1 dysfunction and insulin resistance in rat models of diabetes and obesity. Kidney Int 2011;79:883–896

34. Greenbaum CJ. Insulin resistance in type 1 diabetes. Diabetes Metab Res Rev 2002;18:192–200

35. Leslie RD, Taylor R, Pozzilli P. The role of insulin resistance in the natural history of type 1 diabetes. Diabet Med 1997;14:327–331

36. Yki-Järvinen H, Koivisto VA. Natural course of insulin resistance in type I diabetes. N Engl J Med 1986;315:224–230

37. Ekstrand AV, Groop PH, Grönhagen-Riska C. Insulin resistance precedes microalbuminuria in patients with insulin-dependent diabetes mellitus. Nephrol Dial Transplant 1998;13:3079–3083

38. Coward RJ, Welsh GI, Yang J, et al. The human glomerular podocyte is a novel target for insulin action. Diabetes 2005;54:3095–3102

39. Canaud G, Bienaimé F, Viau A, et al. AKT2 is essential to maintain podocyte viability and function during chronic kidney disease. Nat Med 2013;19:1288–1296

40. El-Osta A, Brasacchio D, Yao D, et al. Transient high glucose causes persistent epigenetic changes and altered gene expression during subsequent normoglycemia. J Exp Med 2008;205:2409–2417

41. Brasacchio D, Okabe J, Tikellis C, et al. Hyperglycemia induces a dynamic cooperativity of histone methylase and demethylase enzymes associated with gene-activating epigenetic marks that coexist on the lysine tail. Diabetes 2009;58:1229–1236

42. Reddy MA, Tak Park J, Natarajan R. Epigenetic modifications in the pathogenesis of diabetic nephropathy. Semin Nephrol 2013;33:341–353

43. Sun G, Reddy MA, Yuan H, Lanting L, Kato M, Natarajan R. Epigenetic histone methylation modulates fibrotic gene expression. J Am Soc Nephrol 2010;21:2069–2080

44. Bock F, Shahzad K, Wang H, et al. Activated protein C ameliorates diabetic nephropathy by epigenetically inhibiting the redox enzyme p66Shc. Proc Natl Acad Sci U S A 2013;110:648–653

45. Advani A, Huang Q, Thai K, et al. Long-term administration of the histone deacetylase inhibitor vorinostat attenuates renal injury in experimental diabetes through an endothelial nitric oxide synthase-dependent mechanism. Am J Pathol 2011;178:2205–2214

46. Wang X, Liu J, Zhen J, et al. Histone deacetylase 4 selectively contributes to podocyte injury in diabetic nephropathy. Kidney Int 2014;86:712–725